ORIGINAL ARTICLE

Journal Section

Collective Behavior of Evaporating Droplets on Superhydrophobic Surfaces

Shiva Moradi Mehr[1] | Luca Businaro[2] | Mehdi Habibi[3] | Ali-Reza Moradi[1,4]

[1] Department of Physics, Institute for Advanced Studies in Basic Sciences, Zanjan, 45195-1159, Iran

[2] Italian National Research Council - Institute for Photonics and Nanotechnologies (CNR - IFN), via Cineto Romano 42, 00156 Rome, Italy

[3]Physics and Physical Chemistry of Foods, Wageningen University, 6700 AA Wageningen, The Netherlands

[4]School of Nano Science, Institute for Research in Fundamental Sciences (IPM), P.O. Box 19395-5531, Tehran, 19395, Iran,

Correspondence
Ali-Reza Moradi, Ph.D., Department of Physics, Institute for Advanced Studies in Basic Sciences, Zanjan, 45195-1159, Iran
Email: moradika@iasbs.ac.ir

Funding information

We study the evaporation dynamics of multiple water droplets deposited in ordered arrays or randomly distributed (sprayed) on superhydrophobic substrates (SHP) and smooth silicone wafers (SW). The evaluation of mass of the droplets as a function of time shows a power-law behavior with exponent 3/2, and from the prefactor of the power-law an evaporation rate can be determined. We find that the evaporation rate on a SHP surface is slower than a normal surface for both single droplet and collection of droplets. By dividing a large droplet into more smaller ones, the evaporation rate increases and the difference between the evaporation rates on SHP and SW surfaces becomes higher. The evaporation rates depend also on the distance between the droplets and increase with increasing this distance.

KEYWORDS
Water evaporation, Droplets, Superhydrophobic surface, Collective behavior

1 | INTRODUCTION

The evaporation of a water droplet is a common phenomenon in nature and has significant applications in technology (e.g. ink-jet printing and surface patterning) [1, 2], biology (e.g. bio-sensing and micro-fluidics) [3, 4, 5], and environmental science (e.g. cooling effect of increased evaporation from trees on the global climate) [6, 7, 8]. Therefore, it

Abbreviations: SHP, Superhydrophobic; SW, Silicon Wafer.

has been subject of intense scientific studies in the recent years [9, 10, 11, 12, 13, 14]. In order to achieve a full picture of the evaporation mechanism many characteristic aspects of it have to be investigated, such as the evaporation rate, flow pattern inside the droplet, air flow, humidity conditions, properties of the surface etc. Picknett and Bexon identified two modes of evaporation for evaporation of a water droplet on a smooth surface; the constant contact angle (CCA) mode and the constant contact line (CCL) mode [15]. In general, evaporation of a single droplet can exhibit a mixed evaporation behavior, often denoted by stick-sliding mode. In CCL mode, the initial contact line remains constant and the contact angle slowly decreases with time. For the CCA mode, the contact line decreases at a fixed contact angle. Dynamics of droplet evaporation clearly depends on the droplet contact angle and therefore, hydrophobicity, contact angle hysteresis, and surface roughness play roles in the evaporation dynamics [16]. Contact line dynamics and wetting transition during evaporation of a single water droplet on a SHP substrate is also investigated in details [17, 13]. It is shown that the higher contact angle of droplet may change the evaporation modes at various stages of the process [16].

In many industrial or environmental applications the evaporation occurs in the presence of other droplets. It is shown recently that evaporation of a collection of droplets on a normal surface is significantly different from single droplet evaporation due to collective effects [10]. The justification is that the surroundings of each droplet are partially saturated by the vapor from the other ones. Therefore, the evaporation rate becomes slower. This collective dynamics in evaporation and overlap of evaporation flux has been studied through a model in which the collection of the droplets has been considered as a super-droplet with the radius obtained from the area covered by the small droplets [10]. In this view, the collective dynamics of multiple droplets evaporating on a SHP surface requires a special attention as it has not been investigated. Here, we investigate the evaporation dynamics of ordered arrays of mono-dispersed and sprayed droplets on SHP and silicone wafer (SW, as a normal substrate) surfaces and address the collective behavior. We also perform single droplet evaporation experiments on both substrates as controlled experiments. We change the droplet size, distance between the droplets and size distribution of sprayed droplets. We also investigate the morphology of droplets during the evaporation and investigate the edge effects for droplets deposited on the edges of an array. Our results might be important for designing self-cleaning surfaces or arrays of droplets for biomedical applications and even environmental applications such as controlling the evaporation rate.

2 | MATERIALS AND METHODS

We used an artificial rough micro-fabricated surface called biomimetic SHP surface, as our SHP substrate. These SHP substrates are made of silicon pillars of 20 μm height and 5 μm side size separated by 14 μm. The SPH areas are fabricated on a silicone wafer (SW) in four different zones of 6 mm$\times$6 mm distanced by 4 mm from each other. The samples are cleaned in piraña solution and functionalized for 24 hrs. The rest of the silicone surface remained unpatterned and used as a normal substrate for comparative study. In Fig. 1 a micrograph of the fabricated sample is shown. We use Mili-Q water as working fluid. Water droplets resting on our SHP surfaces are forced to take an almost spherical shape, with a contact angle higher than 150°. Various configurations of water droplets are made on SHP and SW surfaces (Fig. 1 a-d) by using a micro-syringe. In the first series of experiments the initial total volume of the liquid deposited on the surface is 40 μl. We deposit this amount as a single drop of 40 μl or different combinations of smaller mono-dispersed droplets in form of arrays: two 20 μl, four 10 μl, eight 5 μl and sixteen 2.5 μl as shown in Fig. 1a-d. The experiments were within the limit of slow and quasi-steady evaporation, by keeping the temperature of the system at 22°C throughout the experiments. The experiments are performed in a humidity controlled chamber at a humidity of 50%. The droplet mass variation during the evaporation is measured using a weighting balance (Sartorius,

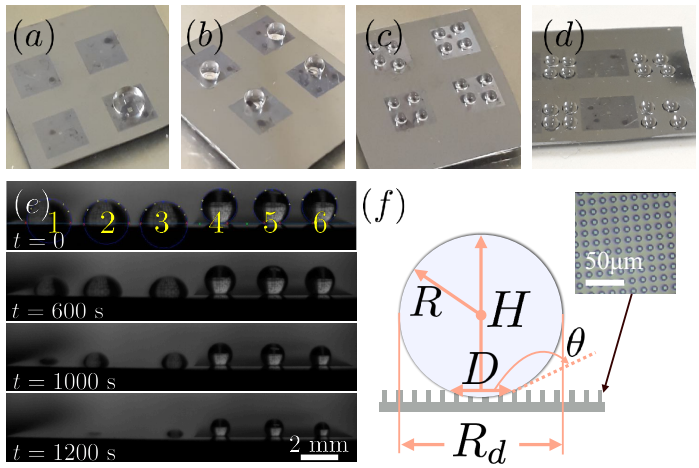

FIGURE 1 The various collection of water droplets of equivalent total mass on the SHP and SW surfaces: (a) 1 droplet of 40 μl, (b) 4 droplets of 10 μl and (c) 16 droplets of 2.5 μl on SHP surface; (d) 16 droplets of 2.5 μl on SW surface; (e) Side view of droplets on SW and SHP substrates to compute morphometric information of droplets in time; (f) Definition of droplet parameters and a micrograph of SHP substrate.

BL 120S) with accuracy of 10^{-4} gr. The experiments are performed on both SHP and smooth SW surfaces. Evolution of the shape of the droplets are captured in some of the experiments by video imaging (DCC1545M, Thorlabs, 8 bit dynamic range, 5.2 μm pixel pitch, at 10 s time intervals). The morphometric parameters of the droplets are measured using image processing of the video sequences. These parameters are defined in the schematic view of the droplet in Fig. 1f. For spray experiments we use a metal fine spray nozzle with minimum drop diameter of about 30 μm. Two different distances of 15 cm and 30 cm between the nozzle and the substrate with different number of puffs are used to achieve different droplet distributions. The SW areas are covered by a mask during the mass measurement in the spray experiments.

3 | EXPERIMENTAL RESULTS AND DISCUSSION

By acquisition of video images from the side view of the evaporating droplets and follow-up image analysis, several morphometric parameters such as contact angle and diameter of contact area can be extracted. In Fig. 2 the time evolution of the contact angle, the contact line, and the height of the 6 droplets of Fig. 1e is shown. The image analysis was performed in MATLAB® by finding the best fitted circle to the 2D images of the side view of the droplets. Data are calculated with a time resolution of 10 s. As one can see in the Fig. 2a evaporation on the both SHP and SW surfaces occurs mainly in CCA mode. The contact angle for the SHP case is $157^\circ \pm 4^\circ$ and for SW surface is $89^\circ \pm 4^\circ$. Only close to vanishing of the droplet the contact angle reduces abruptly to about zero. Diameter of the contact area (D) decreases monotonically for evaporating droplets on the normal surface. This indicates that the contact line is not pined and moves while the contact angle is fixed. As it is clear from Fig. 2b that, the evaporation rate for droplet 1 is higher than droplet 2 and 3 (Fig. 1e) and D of droplet 1 reaches to zero faster than that of the other two. The same behavior is observed for the height (H) of this droplet compared to the other two droplets (Fig. 2c). This is due to the fact that droplet 1 is at the edge of the array while the other two are in between the other droplets. Due to the edge

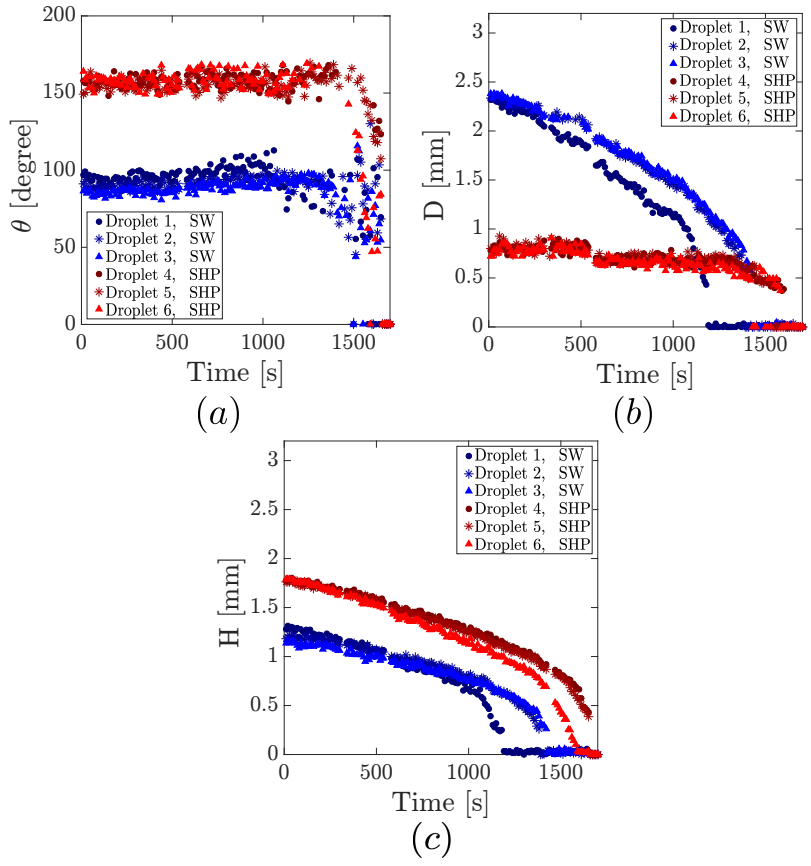

FIGURE 2 Image processing results; Time evolution of (a) contact angle, (b) contact line, and (c) height of the six droplets shown in Fig. 1(e), positioned on SW surface (droplets 1,2, 3) and SHP surface (droplets 4, 5, 6) .

effects the evaporation flux from this droplet is not symmetric and there is a larger flux of evaporation toward the left side of the droplet. In contrast to the SW case, D for evaporation drops on SHP surfaces is roughly constant during the course of evaporation. It shows very slight decrease close to the end and then goes sharply to zero. It has been shown previously for evaporation of a single droplet on a SHP surface, that the contact line shrinks at a much slower rate [17]. On SHP substrates, all evaporation modes may occur; the CCA mode is mostly observed when the contact angle hysteresis is low [18]. D behaves roughly the same for the three droplets on the SHP surface (droplets 4, 5 and 6 in Fig. 1e). Even for droplet 6 deposited at the other edge of the array, D is the same as the other two, however the height (H) of droplet 6 decreases faster than the other two droplets for the same reason as explained above for droplet 1.

Fig. 3a summarizes the time evolution of mass of various collections of droplets evaporating on SHP and SW surfaces in a log-lin scale. Since all the collections have the same initial total mass of 40 mgr all the curves start from this point at time zero. We know that for a small droplet, volume (V) scales as R^3, R being the radius of the droplet, and from $\frac{dV}{dt} \propto R$ [10, 9, 19], it follows that $R \propto (t_f - t)^{1/2}$, where t_f is the total evaporation time. Therefore, it is expected that mass of the droplet changes in power-law in time with an exponent 3/2 as: $m = A(t_f - t)^{3/2}$. Our

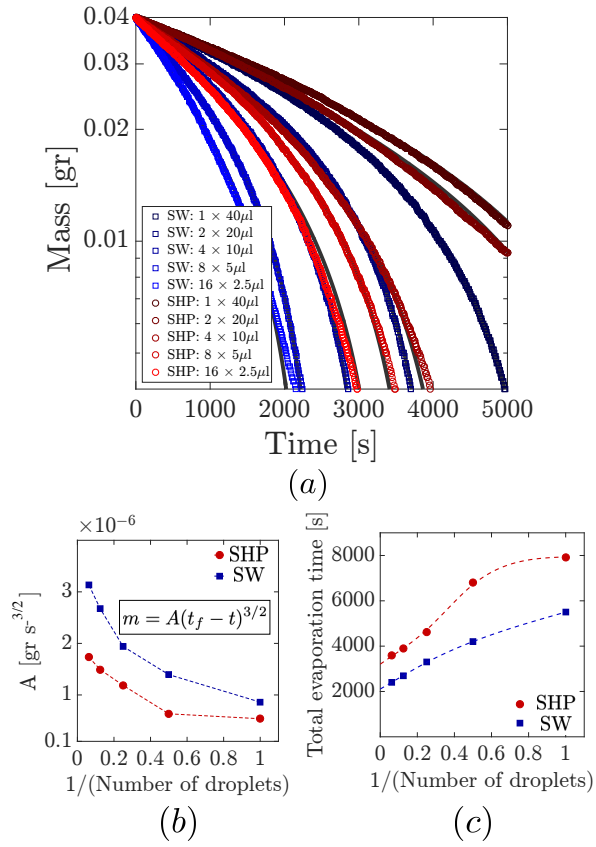

FIGURE 3 (a) Mass as a function of time during the evaporation of various sets of droplets on SHP and SW surfaces; (b) The two-third power fitting pre-factor (A) as a function of inverse of the number of droplets ($1/N$); (c) Total evaporation time as a function of $1/N$.

experimental results confirm 3/2 scaling power for different collections of droplets. Small deviation from the above scaling can be observed at the end of the process. This is mainly due to the fact that the droplets at the edge of the array evaporate faster than the others and vanish before the other droplets, therefore they do not contribute in the final evaporation data. By fitting the above function to our data (solid lines) the pre-factor A for different collections of droplets can be determined. It is known that the pre-factor A depends on the vapor concentration and diffusion coefficient in the atmosphere, the contact line of the droplet, and the density of the liquid [20, 19]. Figure 2b shows the pre-factor A obtained by fitting the data for various collection of droplets as a function of inverse of the number of droplets in the collection ($1/N$). A is higher for evaporation on SW surface than SHP surface. This means that the evaporation on SHP surfaces is slower than the evaporation on SW surfaces. This can be confirmed by looking at the total evaporation time (Fig. 2c). In our experiments, we observed that A increases with up to 3 (2) folds by increasing the number of droplets in the array for the SW (SHP) substrate. Therefore, a collection of small droplets evaporates faster than a single droplet with the same initial mass in agreements with previous studies [9, 10]. This effects is more pronounced for evaporation on the SW surface with respect to SHP surface as shown in Fig. 2c. The main reason for increasing the evaporation rate by reducing the droplet size is due to increasing the total perimeter

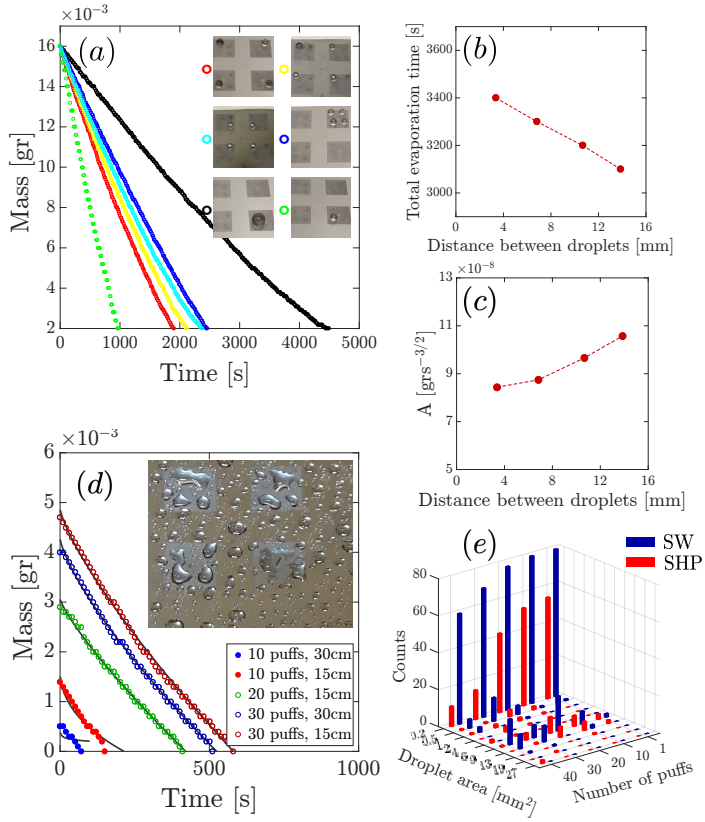

FIGURE 4 (a) The mass of different arrangements of droplets with the same initial mass on a SHP surface as a function of time; (b) The total evaporation time and (c) two-third power fitting pre-factor as a function of the distance between droplets; (d) Total mass as a function of time during the evaporation of sprayed droplets on SHP substrate for various distances and number of puffs; (e) Size distribution of the droplets sprayed from 30 cm for different number of puffs.

of the droplets, since the evaporation rate is proportional to the perimeter of the droplet [9]. However, when the droplets are in closer vicinity of each other, their evaporation flux can overlap and they may partially saturate their surrounding. On the other hand, when the droplets are far away from each other, the influence of their vapor flux on the surrounding droplets suppress and results in faster evaporation. Therefore, the distance between droplets in an array plays an important role on the evaporation dynamics since this distance determines how the evaporation flux can be overlapped. The effect of the distance between droplets in an array on the evaporation rate is demonstrated in Fig. 4a. In this graph, mass of the droplets is shown as a function of time for 6 sets of evaporation on a SHP surface. The total initial volume of droplets for all experiments is 16 μl except the experiments shown by green symbol. The black and green symbols are representing single droplet experiments for 16 and 4 μl droplets, respectively. The mass data for green symbols are multiplied by four to represent four droplets of 4 μl deposited at infinite distance. The single droplet experiments are performed as controlled experiments and showing the slowest (for the 16 μl single droplet) and fastest (for the 4 μl single droplet) evaporation rates. The other four data sets representing the evaporation of four droplets of 4 μl deposited at a center to center distance of 3.4, 6.8, 10.7, and 13.9 mm for dark blue, light blue,

yellow and red symbols, respectively, as shown in the inset of Fig. 4a. The maximum time for evaporation decrease monotonically by increasing the center to center distance between the droplets as shown in Fig. 4b. In addition the parameter A can be determined by fitting 3/2 power-law relation to the data. A represents the evaporation rate and increases by increasing the distance (Fig. 4c). The highest evaporation rate can be achieved when the four droplets are deposited at infinite distance (green symbols in Fig. 4a).

In many real life applications both in technology (e.g. spraying) and nature (e.g. raining) the droplets are distributed with random sizes and distances on a surface. While spraying a liquid, different parameters such as the pressure and geometry of the nozzle, and viscosity and surface tension of the liquid determine the droplet shape and size distribution [21] and consequently affect the evaporation dynamics. The collective dynamics of sprayed droplets on normal surfaces (contact angle$\approx 90^\circ$) have been studied by Carrier et. al. [10] and it is shown that for widely differing size distribution the total mass as a function of time scales like an exponential. To study how the collective dynamics affect the evaporation when the droplets are deposited randomly with random size distribution on a SHP surface, we also measure evolution of the total mass in time (Fig. 4d). We change the distance from the nozzle to the surface and number of puffs which results in different size distributions (Fig. 4e) and initial mass of the droplets on the surface. As expected, by spraying from closer distances or by spraying more puffs larger droplets are deposited on the surface. With respect to SW substrate larger droplets are formed on SHP substrates at similar spraying conditions, as shown in the image of the inset of Fig. 4e. Nevertheless, our experiments demonstrate that the evaporation behavior on SHP surfaces follows a similar exponential trend to the SW surfaces, except in the cases of less puffs from longer spray distances, such as the one shown by filled blue symbols in Fig. 4d.

4 | CONCLUSION

We investigated experimentally the evaporation dynamics of collections of droplets (randomly distributed and ordered arrays) on superhydrophobic surfaces. The results were compared with single droplet evaporation. By tracking the temporal evolution of droplets mass and morphometric video imaging the following conclusions have been drawn from this study:

- For evaporation on a SHP surface the contact area and contact angle of the droplets are constant until the droplet becomes very small. We found that a collection of smaller droplets deposited in an array evaporate faster compared to a single droplet with the same total initial mass, due to increasing the effective perimeter of droplets which provides higher evaporation flux.
- Having another droplet in the neighborhood can decrease the evaporation rate due to overlap of evaporation fluxes. Therefore, increasing the distances between the droplets in an array can increase the evaporation rate by reducing the overlap of the evaporation fluxes.
- In an array of droplets the droplets at the edges evaporate faster due to non-uniform evaporation fluxes which is larger at the empty sides.
- For random distribution of droplets on a SHP surface achieved by spraying from various distances or spraying different numbers of puffs our experiments demonstrate that the evaporation behavior follows a similar trend in all cases in alignment with the results of ordered arrays of droplets.
- Our results indicate that the collective evaporation rate on a SHP substrate is in general lower than that of a normal substrate. These results might provide insight for designing self-cleaning surfaces or droplet arrays for photonics, biological, and medical applications as well as in managing under-evaporation water bodies.

acknowledgements

S. M. M. and A. M. thank Mohammad A. Charsooghi, Maniya Maleki, and Saeid Mollaei for useful discussions.

references

[1] Lim T, Han S, Chung J, Chung JT, Ko S, Grigoropoulos CP. Experimental study on spreading and evaporation of inkjet printed pico-liter droplet on a heated substrate. International Journal of Heat and Mass Transfer 2009;52(1-2):431–441.

[2] Adachi E, Dimitrov AS, Nagayama K. Stripe patterns formed on a glass surface during droplet evaporation. Langmuir 1995;11(4):1057–1060.

[3] Trantum JR, Baglia ML, Eagleton ZE, Mernaugh RL, Haselton FR. Biosensor design based on Marangoni flow in an evaporating drop. Lab on a Chip 2014;14(2):315–324.

[4] Cho SK, Moon H, Kim CJ. Creating, transporting, cutting, and merging liquid droplets by electrowetting-based actuation for digital microfluidic circuits. Journal of Microelectromechanical systems 2003;12(1):70–80.

[5] Javadi A, Habibi M, Taheri FS, Moulinet S, Bonn D. Effect of wetting on capillary pumping in microchannels. Scientific reports 2013;3:1412.

[6] Morton F. Evaporation research - a critical review and its lessons for the environmental sciences. Critical reviews in environmental science and technology 1994;24(3):237–280.

[7] Tanny J, Cohen S, Berger D, Teltch B, Mekhmandarov Y, Bahar M, et al. Evaporation from a reservoir with fluctuating water level: Correcting for limited fetch. Journal of Hydrology 2011;404(3-4):146–156.

[8] Ban-Weiss GA, Bala G, Cao L, Pongratz J, Caldeira K. Climate forcing and response to idealized changes in surface latent and sensible heat. Environmental Research Letters 2011;6(3):034032.

[9] Shahidzadeh-Bonn N, Rafai S, Azouni A, Bonn D. Evaporating droplets. Journal of Fluid Mechanics 2006;549:307–313.

[10] Carrier O, Shahidzadeh-Bonn N, Zargar R, Aytouna M, Habibi M, Eggers J, et al. Evaporation of water: evaporation rate and collective effects. Journal of Fluid Mechanics 2016;798:774–786.

[11] Habibi M, Moller P, Fall A, Rafai S, Bonn D. Pattern formation by dewetting and evaporating sedimenting suspensions. Soft Matter 2012;8(17):4682–4686.

[12] Popov YO. Evaporative deposition patterns: spatial dimensions of the deposit. Physical Review E 2005;71(3):036313.

[13] Chen X, Ma R, Li J, Hao C, Guo W, Luk BL, et al. Evaporation of droplets on superhydrophobic surfaces: Surface roughness and small droplet size effects. Physical review letters 2012;109(11):116101.

[14] Devlin NR, Loehr K, Harris MT. The importance of gravity in droplet evaporation: A comparison of pendant and sessile drop evaporation with particles. AIChE Journal 2016;62(3):947–955.

[15] Picknett R, Bexon R. The evaporation of sessile or pendant drops in still air. Journal of Colloid and Interface Science 1977;61(2):336–350.

[16] McHale G, Aqil S, Shirtcliffe N, Newton M, Erbil HY. Analysis of droplet evaporation on a superhydrophobic surface. Langmuir 2005;21(24):11053–11060.

[17] Gelderblom H, Marin AG, Nair H, Van Houselt A, Lefferts L, Snoeijer JH, et al. How water droplets evaporate on a superhydrophobic substrate. Physical Review E 2011;83(2):026306.

[18] Kulinich S, Farzaneh M. Effect of contact angle hysteresis on water droplet evaporation from super-hydrophobic surfaces. Applied Surface Science 2009;255(7):4056–4060.

[19] Hwang IG, Kim JY, Weon BM. Droplet evaporation with complexity of evaporation modes. Applied Physics Letters 2017;110(3):031602.

[20] Stauber JM, Wilson SK, Duffy BR, Sefiane K. Evaporation of droplets on strongly hydrophobic substrates. Langmuir 2015;31(12):3653–3660.

[21] Kooij S, Sijs R, Denn MM, Villermaux E, Bonn D. What determines the drop size in sprays? Physical Review X 2018;8(3):031019.